J. Chem. Sci. Vol. 129, No. 7, July 2017, pp. 859–872. © Indian Academy of Sciences.
DOI 10.1007/s12039-017-1236-z

CrossMark

REGULAR ARTICLE

Special Issue on THEORETICAL CHEMISTRY/CHEMICAL DYNAMICS

Molecular Dynamics Investigation of Efficient SO_2 Absorption by Anion-Functionalized Ionic Liquids[†]

ANIRBAN MONDAL and SUNDARAM BALASUBRAMANIAN*
Chemistry and Physics of Materials Unit, Jawaharlal Nehru Centre for Advanced Scientific Research, Bangalore 560 064, India
Email: bala@jncasr.ac.in

MS received 19 November 2016; revised 3 January 2017; accepted 16 January 2017

Abstract. Ionic liquids are appropriate candidates for the absorption of acid gases such as SO_2. Six anion-functionalized ionic liquids with different basicities have been studied for SO_2 absorption capacity by employing quantum chemical calculations and molecular dynamics (MD) simulations. Gas phase quantum calculations unveil that the high uptake of SO_2 in these ionic liquids originates from the basicity of the anions and the consequent enhanced anion-SO_2 interactions. MD simulations of SO_2–IL mixtures reveal the crucial role of both cations and anions in SO_2 dissolution. Multiple-site interactions of SO_2 with the anions have been identified. The calculated solvation free energy substantiates these observations. The order of computed Henry's law constant values with change in the anion is in fair agreement with experimentally determined SO_2 solubility order.

Keywords. SO_2 dissolution; ionic liquids; free energy; Henry's law constant.

1. Introduction

Sulfur dioxide (SO_2), a significant air pollutant, is mainly emitted from combustion of fossil-fuel and is a contributor to acid rain.[1] Simultaneously, SO_2 can act as an important intermediate in chemical production.[2] Therefore, it is extremely important to develop novel materials and processes for the efficient removal and possible recovery of SO_2. Although several conventional methods, such as limestone scrubbing and ammonia scrubbing have been developed for flue gas desulfurization (FGD), the inherent drawbacks of these processes should not be neglected, including high energy consumption and wasteful byproducts.[3,4] Recently, ionic liquids (ILs) have drawn immense attention as better acid gas absorbents, owing to their unique properties such as high thermal and chemical stability, negligible vapor pressure, wide liquid range, and tunable chemical properties.[5–12] It was observed that SO_2 has an optimistic solubility in conventional ILs through physical interactions,[2,13,14] and the anion plays a crucial role in its capture.[15,16] Therefore, a new strategy was developed to enhance the absorption capacity of SO_2 at low partial pressure by introducing different weak basic anions to form anion-functionalized ILs. Wu *et al.*, first reported the task-specific IL, 1,1,3,3-tetramethylguanidinium lactate ([TMG][L]) that absorbs an equimolar amount of SO_2 through chemisorption.[12] Subsequently, a significant number of task-specific ILs were designed and used to capture and separate SO_2.[2,13,17–29]

The electronegative oxygen or nitrogen site in the anion of task-specific ILs possesses very strong interaction (Lewis acid-base type) with the SO_2 molecule leading to its chemisorption.[14,30,31] Thus, the chemical absorption process results in a high uptake of SO_2. However, as a consequence, the desorption gets difficult, making the gas regeneration process expensive.[32,33] To reduce the absorption enthalpy, several techniques were developed, such as tuning the basicity[34] and introduction of an electron-withdrawing group on the anion.[35–37] However, these approaches most often result in a reduced absorption capacity, due to diminished interaction strength between the gas and the IL.

Recently, Wang *et al.*, demonstrated a new strategy for efficient SO_2 absorption and facile desorption by introducing an electron withdrawing site on the anion in anion-functionalized ILs.[26,31,32,38–44] The motivation behind this strategy was three-fold: a) increase in the SO_2 absorption capacity, b) reducing the absorption enthalpy for easy desorption and c) efficient capture of SO_2 at very low concentration (about 2000 ppm). The electron-withdrawing group diminishes the absorption enthalpy, which in turn improves the desorption and subsequently, it acts as an added interaction site that increases absorption capacity. These ILs exhibited very

*For correspondence
[†]Dedicated to the memory of the late Professor Charusita Chakravarty

high absorption capacity, ± 4.5 mol SO_2 per mole of IL through multiple-site interactions.

Molecular simulations have been crucial on several occasions to obtain microscopic insights behind gas absorption in ILs.[45–62] Perez-Blanco and Maginn demonstrated the formation of a dense layer of CO_2 molecules at the interface of 1-*n*-butyl-3-methylimizazolium bis(trifluoromethylsulfonyl)imide ([BMIM][NTf_2]) by MD simulations.[63] Dang *et al.* and Siqueira *et al.*, examined the nature of interactions of CO_2 and SO_2 at the air/liquid interface through solvation free energy.[64,65] *Ab initio* calculations based on density functional theory (DFT) have shown that interactions of ILs with SO_2 are stronger than those with CO_2 and N_2.[15] Further, it was seen that anions dominate the interactions with gas molecules and the cations play only a minor role.[15,16]

Although simulation studies of CO_2 capture by ILs are numerous, not much attention has been devoted to SO_2 absorption in ILs,[15,59,60,65] especially, in task-specific ILs.[54] Discerning the mechanism of multiple-site interactions between the anion and SO_2 which results in a dramatic increase of absorption capacity with low absorption enthalpies is of extreme importance. In this spirit, the present work is devoted to understand the microscopic interactions and consequent effect on SO_2 capture by six anion-functionalized ILs using MD simulations and quantum chemical calculations.

2. Computational details

Task-specific ILs consisting of various functionalized anions were considered in this work. Experiments on SO_2 solubility in ILs have been carried out by Wang *et al.,* with $[P(C_6H_{13})_3C_{14}H_{29}]^+$ as the cation.[39,41,42] In order to reduce computational cost, the present work utilizes $[P(C_2H_5)_3CH_3]^+$ or $[P_{2221}]^+$ as the common cation in combination with anions such as, $[4\text{-}BrC_6H_4O]^-$, $[4\text{-}BrC_6H_4COO]^-$, $[4\text{-}CNC_6H_4O]^-$, $[4\text{-}CNC_6H_4COO]^-$, $[Tetz]^-$ and $[DCA]^-$. These are displayed in Figure 1. Wang *et al.*, reported the solubility of SO_2 in $[P(C_6H_{13})_3C_{14}H_{29}]^+$ based functionalized ILs to be in the order $[BrPhCOO]^- > [CNPhCOO]^- > [Tetz]^- > [CNPhO]^- > [BrPhO]^- > [DCA]^-$.[39,41,42]

2.1 *Quantum chemical calculations*

DFT calculations were performed with Gaussian 09 program[66] at M06/aug-cc-pVDZ level of theory. Geometry optimization of isolated IL ion pair, SO_2 molecule, and SO_2–IL complex (one SO_2 molecule and one IL ion pair each) were carried out. GaussView software[67] was utilized to construct the initial configurations, wherein SO_2 molecule was placed at six different locations around the IL ion pair such as phenolate oxygen, carboxylate oxygen, bromine, cyano group, N_A, N_B, H_A, etc. Results presented here pertain to the lowest energy configuration selected among these optimized geometries. Frequency analysis confirmed the minimum energy configuration. Binding energy (BE) was computed as

$$BE = E_{SO_2-IL} - (E_{IL} + E_{SO_2}) + E_{BSSE} \qquad (1)$$

where E_{SO_2-IL}, E_{IL}, E_{SO_2}, and E_{BSSE} represent the energy of SO_2–IL complex, IL ion pair, SO_2, and the counterpoise correction for basis set superposition error (BSSE),[68] respectively. Further, to gain better insight into the contributions to the interaction energy of the SO_2–IL complexes, we performed Symmetry Adapted Perturbation Theory (SAPT) calculations[69] using PSI4 software.[70] Minimum energy configurations

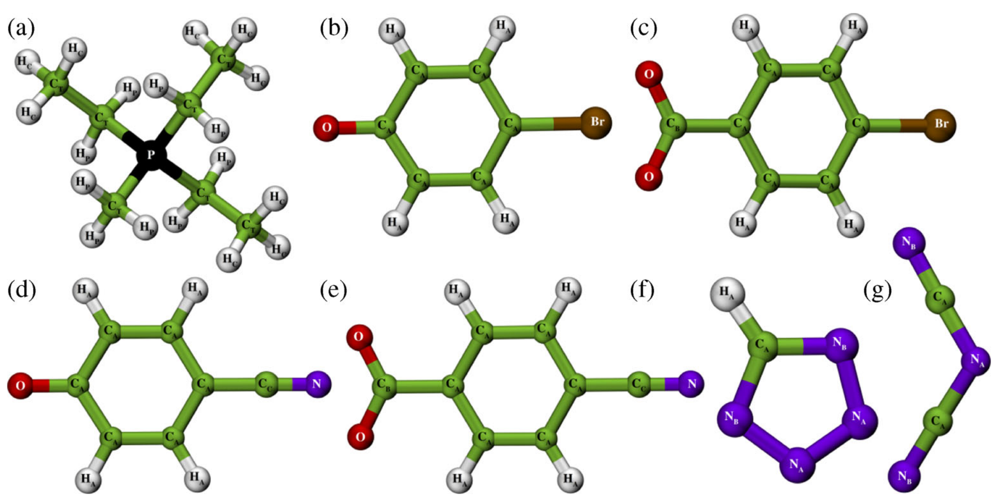

Figure 1. Molecular structure of a) $[P_{2221}]^+$, b) $[BrPhO]^-$, c) $[BrPhCOO]^-$, d) $[CNPhO]^-$, e) $[CNPhCOO]^-$, f) $[Tetz]^-$ and g) $[DCA]^-$ used in simulations. Color scheme: phosphorus, black; carbon, green; hydrogen, white; oxygen, red; nitrogen, blue; bromine, ochre.

at M06/aug-cc-pVDZ level were exploited in the SAPT2[71] calculations.

2.2 *Classical MD simulations*

MD simulations were performed with the LAMMPS program.[72] Force field parameters for $[P_{2221}]^+$ cation were adopted from the work of Wang *et al.*,[73] while anions were modelled using the all-atom TraPPE parameters.[74,75] Atomic site charges for these functionalized ILs were obtained following the protocol described elsewhere[76,77] and a detailed description is given in the Supplementary Information (SI). The fully flexible SO_2 molecule was modelled with parameters previously used in simulation of neat SO_2 and of SO_2 in ILs.[60,65,78] Cross interactions were handled using Lorentz-Berthelot rules. Long-range Coulombic interactions were treated using the particle-particle particle-mesh solver. Long-range corrections to energy and pressure were applied. Equations of motion were integrated using velocity Verlet algorithm with a time step of 1 fs. All C–H covalent bonds were constrained using SHAKE algorithm as implemented in LAMMPS.[72] Additionally, simulations were performed for systems such as $[P(C_6H_{13})_3C_{14}H_{29}]$ [BrPhO] and $[P(C_6H_{13})_3C_{14}H_{29}]$[BrPhCOO] to validate the force field. The density of these two ILs (as the experimental density values for other ILs are not available) computed at 298 K are compared against experimental values[39] as shown in Table S1 (see SI). A satisfactory agreement between experimental and simulated data is observed, with a maximum deviation of 1%.

Experimental measurements suggest that the solubility of SO_2 in ILs with multiple site interactions is higher than one mol per mol of IL.[39,41,42] Thus, in the case of bulk simulations, 256 cations, 256 anions and 256 SO_2 molecules were placed in a cubic box to attain equimolar concentration. The starting configurations were generated with the program Packmol.[79] For all the mixtures considered, starting configurations were subjected to energy minimization followed by 10 ns equilibration in the isothermal-isobaric (NPT) ensemble at 1 atm and 298 K. The temperature and pressure were maintained *via* Nosé-Hoover thermostat and barostat.[80,81] Subsequently, all the systems were equilibrated in NVT ensemble for 5 ns, followed by a 40 ns production run in the NVT ensemble. The box lengths for pure IL and SO_2–IL mixture are provided in Table S2 of SI. VMD[82] was used for visualization.

2.3 *Free energy calculations*

Free energy (FE) profiles were obtained using the "colvars" module[83] as implemented in LAMMPS.[72] Adaptive Biasing Force (ABF)[84] method was employed to determine the FE profiles. The IL configuration for these simulations was generated as follows: 256 ion pairs were equilibrated in a cubic box in the NPT ensemble at 298 K for 10 ns. The cell length along the z-axis was later stretched to 200 Å which created two liquid-vapor interfaces and the system was further equilibrated for 2 ns in NVT ensemble. Subsequently, FE calculations were performed in the NVT ensemble. The reaction coordinate (RC) was defined as the distance between the center of mass (COM) of the IL and the center of mass of the SO_2 molecule (Figure S1 in SI). Solvation free energy (SFE) is the energy required to bring one SO_2 molecule from the gas phase into the bulk IL. The RC spanned from 0 Å (center of IL box) to 60 Å and was divided into four nonoverlapping windows. The colvar style of "distanceZ" was used to determine the free energy profiles. ABF forces were applied every 500 steps with a bin width of 0.1 Å. In each window, an average sampling ratio of 5 between the highest and lowest point was achieved, after running for at least 40 ns.

3. Results and Discussion

3.1 *Quantum chemical analysis*

An investigation of various intermolecular interactions between the gas and the ILs can be undertaken to understand SO_2 uptake in these ILs. Figure 2 displays the minimum energy structures of the SO_2–IL complexes. The molecular structure of SO_2 was seen not to be perturbed by its interactions with IL ions.

3.1a *Ion pair-SO_2 structure*: The interaction of SO_2 with these functionalized ILs can be broadly classified into two types: a) strong Lewis acid-base interaction with the anion, where the most electron rich sites on anion (either oxygen or nitrogen) share their electron density with the sulfur atom in SO_2, and b) weak hydrogen bond interactions with various C–H hydrogens in the cation. Anions with high basicity, such as $[BrPhO]^-$ and $[CNPhO]^-$, interact strongly with SO_2, as evident from the shortest S–O (anion) distance (1.98 Å) in the respective SO_2–IL complexes (Figure 2). Less basic anions, e.g., $[BrPhCOO]^-$ and $[CNPhCOO]^-$ are slightly farther away from sulfur (2.16 Å and 2.19 Å, respectively). However, in the case of $[Tetz]^-$, the gas molecule not only interacts with the electron rich nitrogen center (S–N_B distance; 2.19 Å) in the anion but also possesses a strong hydrogen bond with anion H_A atom (O–H_A distance; 2.01 Å). On the other hand, $[DCA]^-$, the least basic among these anions, interacts with the gas molecule from the farthest distance (S–N_B

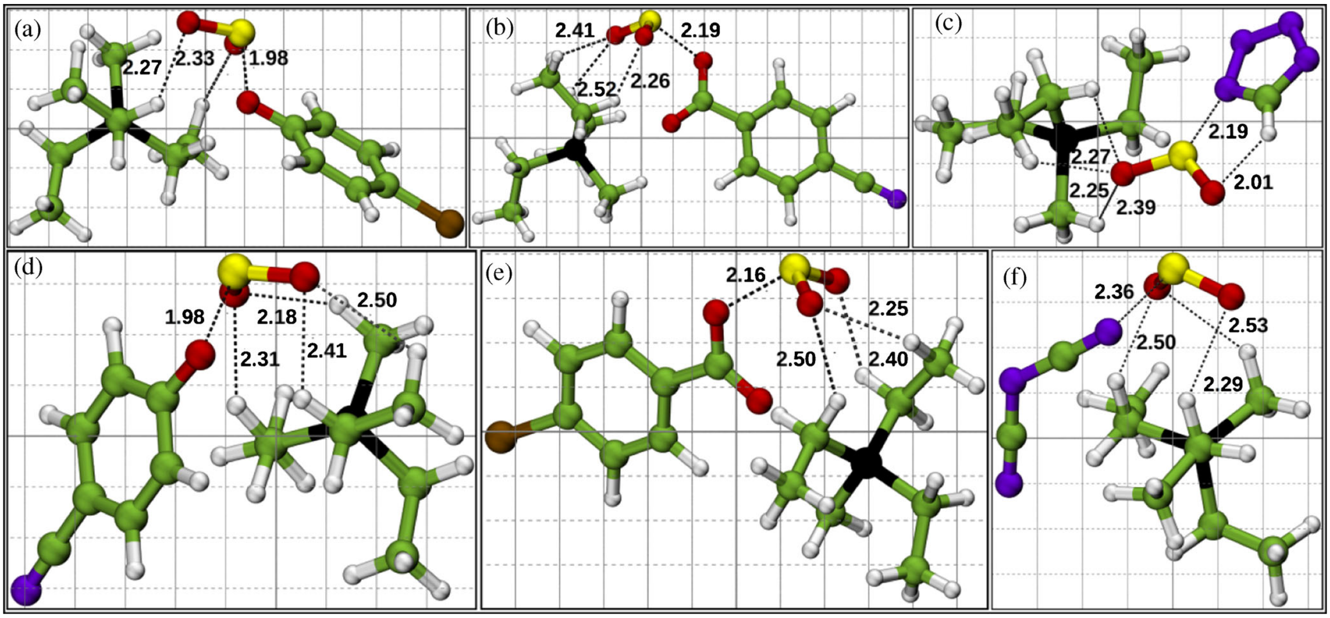

Figure 2. Minimum energy structures of the complexes of SO_2 with a) [P_{2221}][BrPhO], b) [P_{2221}][CNPhCOO], c) [P_{2221}][Tetz], d) [P_{2221}][CNPhO], e) [P_{2221}][BrPhCOO] and f) [P_{2221}][DCA] obtained from gas phase, quantum chemical calculations. Dotted lines are interatomic distances in Å.

Table 1. Binding energies (BE, kcal/mol) at M06/aug-cc-pVDZ level of theory and energy decomposition of the interaction energy (kcal/mol) at SAPT2/aug-cc-pVDZ level of theory of SO_2–IL complexes. The last two complexes are provided to identify the effect of Br and CN substitutions in the first and the third complexes.

SO_2–IL complex	BE	E_{SAPT2}	E_{elst}	E_{exch}	E_{ind}	E_{disp}
[P_{2221}][BrPhO]	−54.18	−58.54	−137.81	216.27	−105.12	−31.88
[P_{2221}][BrPhCOO]	−41.75	−43.81	−100.47	153.61	−67.20	−29.75
[P_{2221}][CNPhO]	−50.03	−52.39	−111.46	172.88	−86.70	−27.11
[P_{2221}][CNPhCOO]	−38.62	−40.34	−82.19	119.77	−52.55	−25.37
[P_{2221}][Tetz]	−48.27	−50.62	−118.06	187.75	−89.21	−31.10
[P_{2221}][DCA]	−29.88	−31.92	−61.77	93.76	−39.73	−24.18
[P_{2221}][PhO]	−65.89	–	–	–	–	–
[P_{2221}][PhCOO]	−47.48	–	–	–	–	–

distance; 2.36 Å). In each of these SO_2–IL complexes, the oxygen atom of SO_2 forms a hydrogen bond with the cation hydrogen atoms *e.g.*, H_P or H_C, irrespective of the basicity of the anions. This observation reflects on the role of cations in SO_2 dissolution in these functionalized ILs.

3.1b *Interaction energy*: The binding energies (BE) at M06/aug-cc-pVDZ level of theory for SO_2–IL complexes were computed to reaffirm the order of the strength of SO_2 interaction with ILs. These energies are tabulated in Table 1. Among all the ILs, [P_{2221}][BrPhO] exhibits the highest affinity in binding to SO_2, followed by [P_{2221}][CNPhO] and [P_{2221}][Tetz]. The highly basic nature of the phenoxide anions allows them to form stronger SO_2–IL complex that results in a large value of absorption enthalpy, whereas in [P_{2221}][Tetz], the presence of both Lewis acid-base interaction and strong hydrogen bond with anion contribute to the higher binding energy. Due to the more electron withdrawing nature of cyano group in comparison to bromine, the electron density at phenoxide oxygen atom is lesser in the cyano substituted anion, which reduces the BE for the SO_2-[P_{2221}][CNPhO] complex relative to that in the [BrPhO] system. Moreover, the lower basicity of benzoate anions and $[DCA]^-$ manifested in their lower BE values for SO_2–IL complex. In phenoxide and benzoate anions, minimum energy configuration was the one where the SO_2 molecule interacts with the anion oxygen atom (Figure 2). In principle, the SO_2 molecule can also interact with either the bromine or cyano group in these anions. The optimized geometry obtained when the SO_2 molecule was kept near those groups was found to be 3–4 kcal/mol less stable than the minimum energy configuration. For the sake of comparison, we have also computed the binding energy of SO_2-[P_{2221}][PhO] and

SO_2-[P_{2221}][PhCOO] complexes at the same level of theory. It is evident from Table 1 that in the absence of any functionalization at para position, both phenoxide and benzoate anions exhibit much stronger interaction with the solute SO_2 molecule. However, both bromine and cyano group reduce the binding energy by a significant amount. Thus, on the one hand, these electron withdrawing groups act as an additional site for SO_2 binding (which increases the SO_2 absorption capacity), while on the other hand, they result in lower interaction energy *i.e*., diminished absorption enthalpy.

3.1c *Energy decomposition analysis*: In order to discern the nature of interaction of SO_2 with the ILs, the total interaction energy for each of this SO_2–IL complex was decomposed into individual contributions and these too are provided in Table 1. Dispersion (E_{disp}) contributes more than 50% towards the total interaction energy. Contribution from the electrostatic energy (E_{elst}) is significant in the complexes with highly basic anions, while dispersion energy (E_{disp}) contributes maximum (75%) in complex with weak basic [DCA]$^-$ anion. Thus, dispersion forces are of immense importance for the efficient absorption of SO_2 in these ILs.

3.2 *Liquid structure*

3.2a *Ion-ion g(r)*: The influence of SO_2 on the bulk liquid structure was elucidated by studying the structural correlations between cations and anions computed from the MD trajectories of pure IL and SO_2–IL mixtures. The radial distribution functions (RDFs) between cation-anion, H_P-anion, and H_C-anion in the pure IL and SO_2 loaded ILs are displayed in Figure S2 of SI. It is evident that the structure of these ILs remain unaltered even in the presence of the solute.[56,57,60,85]

3.2b *SO_2-ion g(r)*: Several experiments[39,41,42,86] and molecular simulation[15,16,60] studies exhibited that the nature of anions has a profound effect on the interaction between SO_2 and ILs. Figure S3 (in SI) shows the RDFs between the center of mass (COM) of the ions and that of SO_2. As shown in Figure S3b (in SI), SO_2 is predominantly located near the [DCA]- anion, as evidenced by the short peak around 3.8 Å, followed by small hump around ± 5.1 Å in [P_{2221}][DCA]. Similarly, in [P_{2221}][Tetz], we can see a clear shoulder at 3.7 Å, which is followed by a sharp peak near 4.1 Å. However, in the case of the larger phenoxide and benzoate based anions, the first peak in SO_2–anion g(r) are present at a slightly large distance. These RDFs also exhibit a hump at small distances (3.5 Å). The presence of multiple peaks and a broad first peak demonstrate that SO_2 interacts with multiple sites of the anions in these SO_2–IL complexes. We have examined the SO_2-anion interactions in more detail through various site-site RDFs.

3.2b1 *SO_2-anion site (O/N/Br) g(r)*: Figure 3 displays RDFs between the sulfur atom of SO_2 and two electron rich centers in the anion, such as O and N/Br site in phenoxide and benzoate anions; and N_A and N_B sites in [Tetz]$^-$ and [DCA]$^-$ (Figure 1). Electron rich oxygen centers in phenoxide and benzoate anion (higher basicity) interact strongly with SO_2 at shorter distances than less electron rich nitrogen sites in either [Tetz]$^-$ or [DCA]$^-$ anion (lower basicity) (see Figure 3a). The coordination numbers (integrated up to first minimum of the corresponding radial distribution function) suggest that SO_2 is surrounded by more number of oxygen atoms in benzoate anions (2.3) than in phenoxide anions (0.70), whereas more number of N_B atoms are observed around SO_2 in [P_{2221}][DCA] (3.9) than in [P_{2221}][Tetz] (3.5). On the other hand, the cyano group exhibits stronger interaction with the solute SO_2 than bromine, as is evident from Figure 3b. Phenoxide anion is more basic than benzoate and cyano group has more electron withdrawing capability than bromine; thus, the electron density at para substituted group in [CNPhO]$^-$

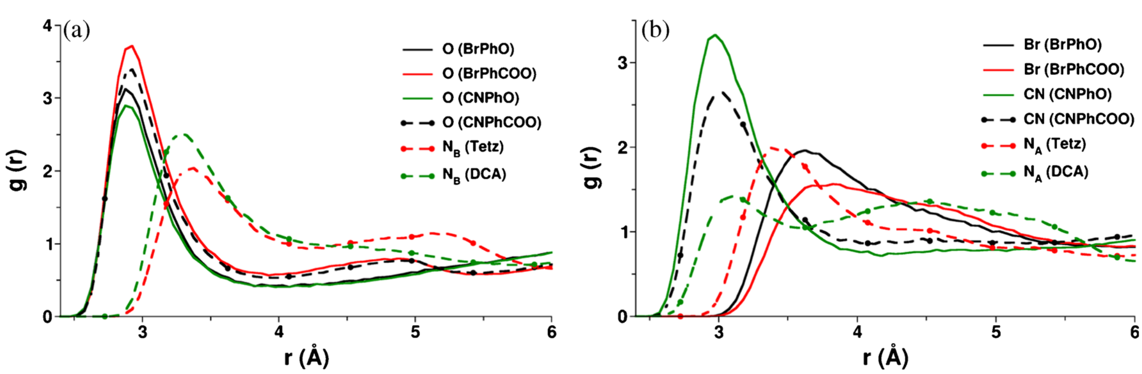

Figure 3. Radial distribution functions between various sites in anion and SO_2 in SO_2–IL mixtures. [P_{2221}]$^+$ is the common cation.

is maximum, followed by $[CNPhCOO]^-$, $[BrPhO]^-$, and $[BrPhCOO]^-$. A similar order is observed in the first peak position in RDFs of these groups with SO_2 and their corresponding coordination numbers. Moreover, the N_A sites in $[Tetz]^-$ and $[DCA]^-$ also possesses significant interaction with SO_2, as can be seen from peaks present between 3–3.5 Å distance, although the coordination numbers suggest that SO_2 is surrounded by very few N_A atoms. Thus, SO_2 prefers to bind more towards the more electron rich oxygen centers in phenoxide and benzoate anions and N_B sites in $[Tetz]^-$ and $[DCA]^-$, consistent with the preference seen in gas-phase quantum chemical calculations, discussed earlier.

3.2b2 $SO_2{-}H_P/H_C\,g(r)$: Further, we have examined RDFs between various hydrogen atoms on the cation and anion with SO_2 oxygens to demonstrate the contribution of these specific interactions in SO_2 dissolution and these are presented in Figure S4 (in SI) and Figure 4. The H_C atoms on the cation exhibit stronger interaction with SO_2 than H_P atoms do as is evident from well-defined and sharp peak around 2.8 Å for the former, see Figure 4a. Moreover, the first peak height in SO_2–H_P g(r) (2.7 Å, see Figure S4, in SI) is lower than that of SO_2–H_C g(r). The coordination numbers indicate that SO_2 is surrounded by more number of H_C atoms (1.6) than H_P atoms (0.95). Thus, the SO_2

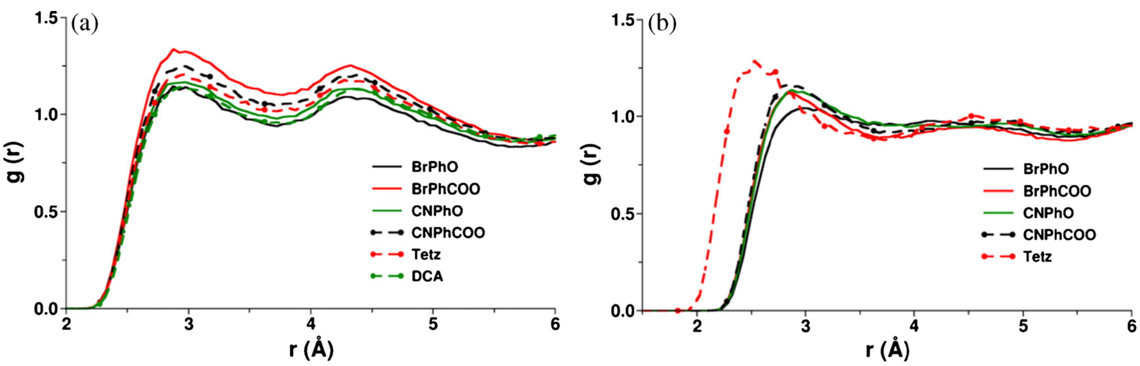

Figure 4. Radial distribution functions between a) O–H_C and b) $O(SO_2)$–H_A in SO_2–IL mixtures. $[P_{2221}]^+$ is the common cation.

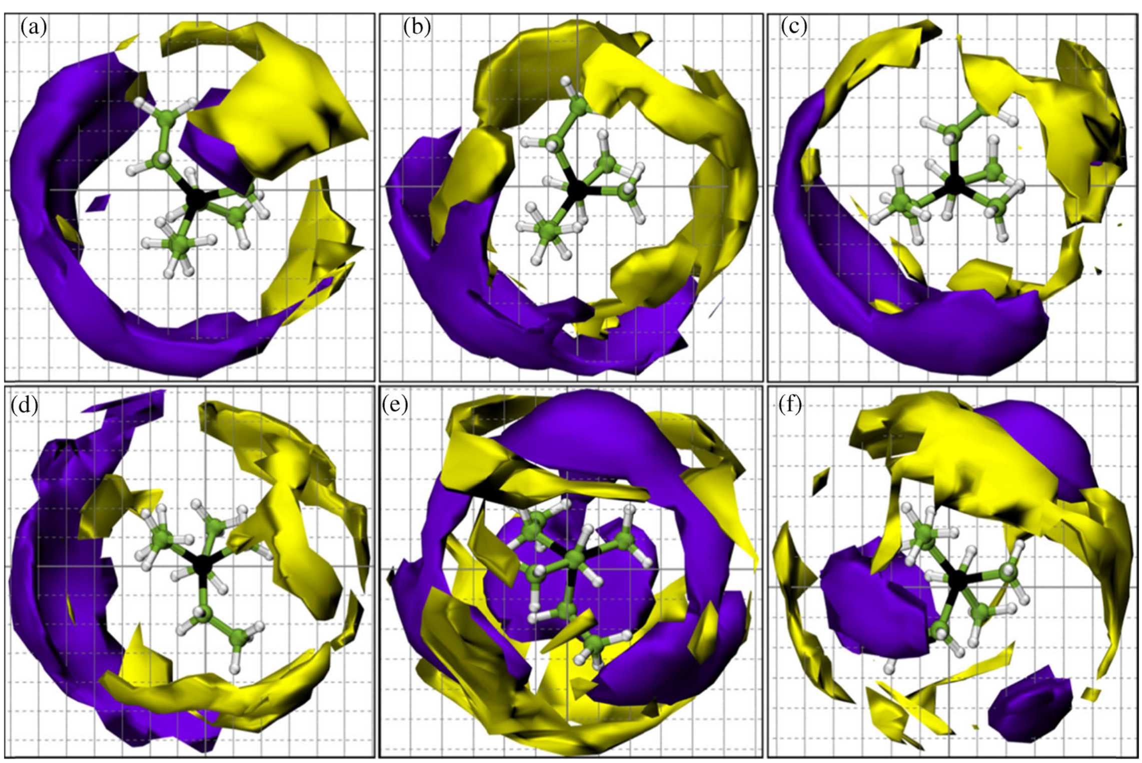

Figure 5. Spatial density map of anion (purple) and SO_2 (yellow) around the center of mass of the cation for a) $[BrPhO]^-$, b) $[BrPhCOO]^-$, c) $[CNPhO]^-$, d) $[CNPhCOO]^-$, e) $[Tetz]^-$ and f) $[DCA]^-$. Isosurface density: 0.006 $Å^{-3}$. Color scheme: black, phosphorus; green, carbon; white, hydrogen.

molecule interacts with cation *via* strong interaction with alkyl H_C atoms and consequently, it denotes the importance of dispersion forces in SO_2 solubility in these ILs as was earlier noted in SAPT calculations and earlier studies.[57,60]

3.2b3 SO_2–$H_A g(r)$: Figure 4b presents the RDFs between anion hydrogen atoms (H_A) and SO_2 oxygen atoms. Similar to H_C atoms, H_A sites also possess a strong interaction with SO_2, indicated by well defined peak around 2.85 Å in phenoxide and benzoate based ILs. Interestingly, a very strong interaction at much shorter distance (2.4 Å) is observed between H_A and SO_2 in $[P_{2221}]$[Tetz], which was also seen in the gas phase DFT calculations (O(SO_2)–H_A distance, 2.0 Å). H_A atom in $[Tetz]^-$ is covalently bonded to a carbon atom which sits in between two electronegative nitrogen atoms. Thus the acidity of the H_A atom in $[Tetz]^-$ is larger than in phenoxide or benzoate anions. As a result, among all the anions studied here, SO_2 exhibits stronger hydrogen bond interaction with [Tetz]-. In summary, multiple-site interactions between the anion and SO_2 explain the extremely high SO_2 absorption capacity in these anion-functionalized ILs.

Furthermore, these structural correlations were validated by computing spatial distribution functions (SDFs)[60,76,77] in SO_2 loaded ILs. The SDFs calculated for the anion and SO_2 around the center of mass (COM) of the $[P_{2221}]^+$ cation are shown in Figure 5. The density map of anions around the COM of cation shows that anions tend to bind to the H_P hydrogen atoms located on the first carbon in alkyl chain rather than H_C sites. A similar preference for H_P atoms over H_C atoms was also observed in their respective RDFs (see Figure S2, in SI.) Around the cation, the SO_2 density map is more condensed over the H_C atoms with some scattered density around H_P sites too. These observations are agreement with the RDF analysis and gas phase DFT calculations.

Figure 6 displays the computed SDFs of the cation and SO_2 molecule around the center of mass of the anion, at an isosurface value of 0.006 Å^{-3}. It is evident that SO_2 is closer to the anion than to the cation, an observation which is consistent with the RDFs as well (see Figure S5, in SI). SO_2 shows stronger binding preference towards the more electron rich centers in the anion; *e.g.*, oxygens in phenoxide or benzoate anions and nitrogens in others. Besides this, significant interactions are observed between SO_2 and other additional

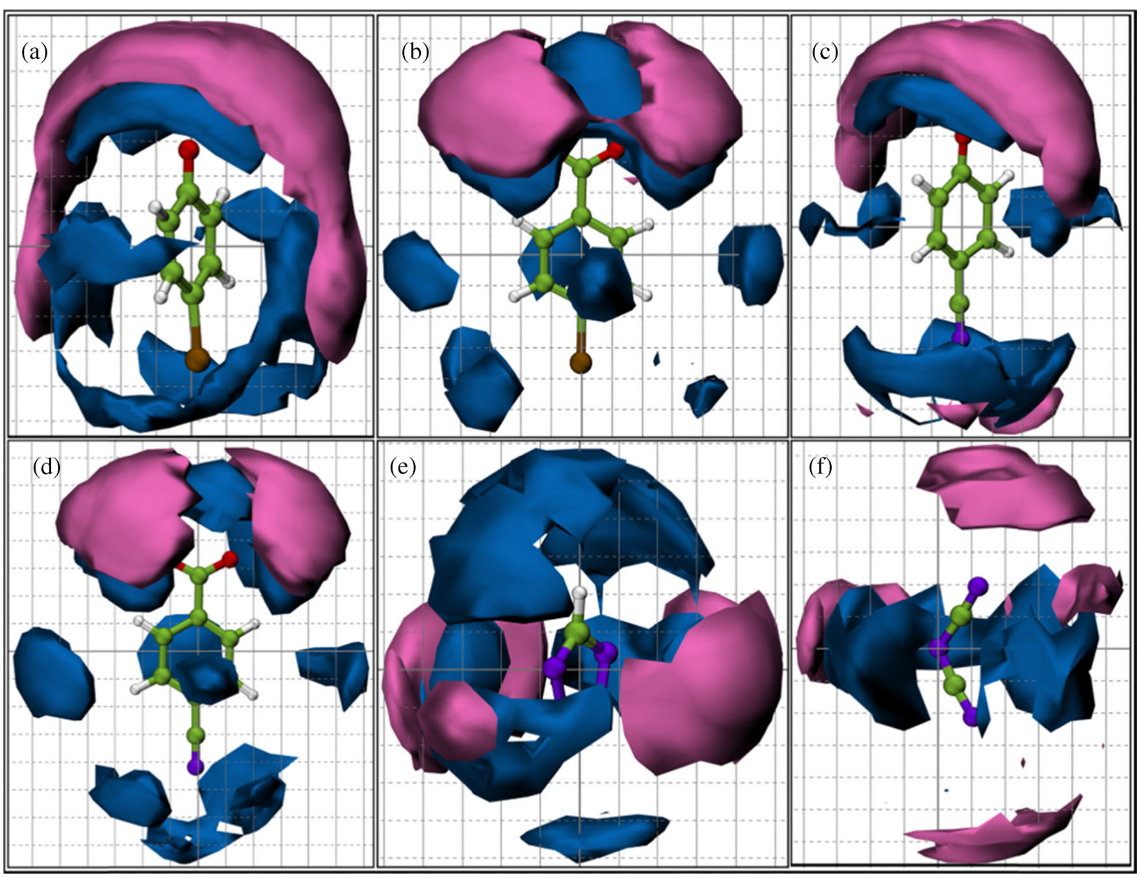

Figure 6. Spatial density map of cation (pink) and SO_2 (blue) around the center of mass of the anion for a) $[BrPhO]^-$, b) $[BrPhCOO]^-$, c) $[CNPhO]^-$, d) $[CNPhCOO]^-$, e) $[Tetz]^-$ and f) $[DCA]^-$. Isosurface density: 0.006 Å^{-3}. Color scheme: green, carbon; white, hydrogen; red, oxygen; violet, nitrogen; ochure, bromine.

sites in the anion such as bromine, cyano group, and H_A atoms. The strength of this additional interaction can be rationalized in terms of available electron density at those additional sites. In this regard, phenoxide group is more basic in nature than the benzoate group; and while bromine is a moderate electron withdrawing group, cyano group exhibits a strong electron withdrawing nature. Thus, electron density at the para substituted group can be ordered as, $[P_{2221}]$[CNPhO], $[P_{2221}]$[CNPhCOO], $[P_{2221}]$[BrPhO] and $[P_{2221}]$[BrPhCOO]. As a consequence, SO_2 binds more strongly to the cyano group in $[P_{2221}]$[CNPhO] or $[P_{2221}]$[CNPhCOO], than to the bromine sites in $[P_{2221}]$[BrPhO] or $[P_{2221}]$[BrPhCOO], as evident from a more condensed density of SO_2 near the cyano group. Also, SO_2 density was found near the H_A atoms, indicating a binding preference for SO_2 with this site. Especially, in $[P_{2221}]$[Tetz], the density map of SO_2 is highly condensed around H_A atom. These observations substantiate further the conclusions drawn from RDF analysis and gas phase quantum chemical calculations and demonstrate the importance of multiple site interactions in high uptake of SO_2 in these task-specific ILs.

Combined distribution functions (CDFs)[87,88] were computed to demonstrate the arrangement of cations and SO_2 around the anion ring plane and the same are shown for $[P_{2221}]$[CNPhO] and $[P_{2221}]$[Tetz] in Figures 7 and 8, respectively (see Figures S6–S8 in SI for such data for other ILs). As discussed earlier, H_P atom exhibits predominant interaction with anion while SO_2 prefers to bind near the H_C atom. Figures 7a and 8a show the strong interaction of anion with the H_P site, while preferable interaction of SO_2 with the H_C atoms is evident from Figures 7c and 8c, in these ILs. Similar phenomenon was also observed in other ILs as shown in Figure S6–S8 in SI. The CDF (Figure 7b) exhibits that $[P_{2221}]^+$ cation prefers an in-plane arrangement with the anion ring rather than the on-top arrangement in $[P_{2221}]$[CNPhO] (similar orientation was also observed for other phenoxide- and benzoate-based ILs, as shown in Figures S6–S8 in SI). However, in $[P_{2221}]$[Tetz], $[P_{2221}]^+$ cation is observed to be both at in-plane and on-top arrangements (Figure 8b). This phenomenon can be justified in terms of cation's preference to bind at electronegative oxygen sites in phenoxide- and benzoate-based ILs. However, the orientation of SO_2 molecule

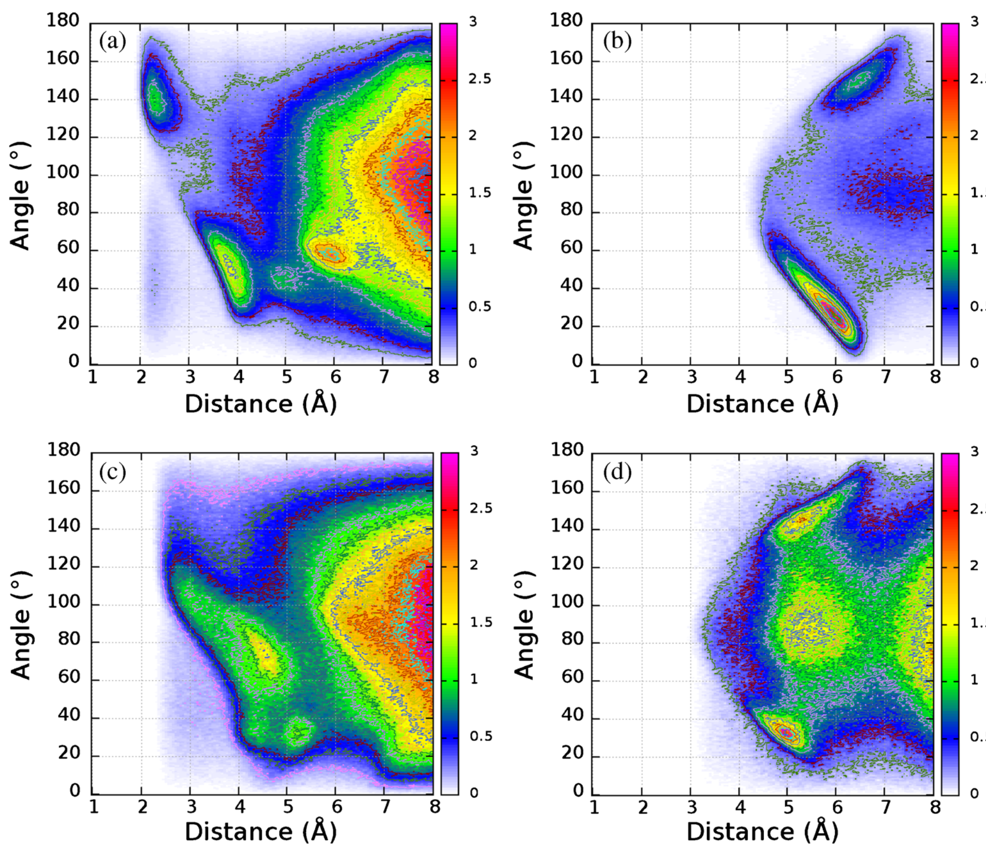

Figure 7. Combined distribution functions depicting the in-plane and on-top distribution with relative intensity color coding. The distance is a) H_P-anion, b) CoR-CoM (cation), c) H_C-SO_2 and d) CoR-CoM (SO_2). The angle is a) C_T-H_P-anion, b) CoR-C_A-CoM (cation), c) C_T-H_C-SO_2 and d) CoR-C_A-CoM (SO_2). CoR indicates the center of the benzene ring and CoM, the center of mass of either the cation or of SO_2. The anion is $[CNPhO]^-$.

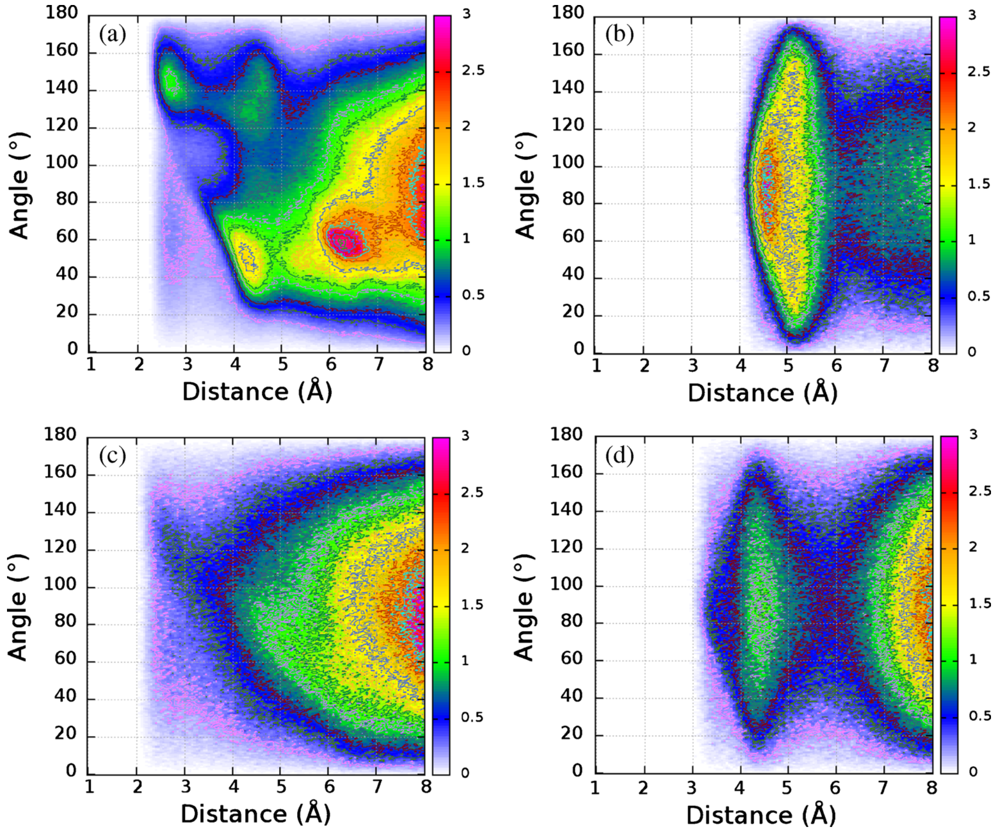

Figure 8. Combined distribution functions depicting the in-plane and on-top distribution with relative intensity color coding. The distance is a) H_P-anion, b) CoR-CoM (cation), c) H_C-SO_2 and d) CoR-CoM (SO_2). The angle is a) C_T-H_P-anion, b) CoR-C_A-CoM (cation), c) C_T-H_C-SO_2 and d) CoR-C_A-CoM (SO_2). CoR indicates the center of the triazole ring and CoM center of mass of either cation or SO_2. The anion is $[Tetz]^-$.

around the anion ring plane is independent of the anion, as the SO_2 molecule is seen at both the on-top and in-plane locations (Figures 7d and 8d). These observations further validate the multiple-site interactions of SO_2 with anions, which were also seen in RDF and SDF analyses.

3.3 *Solvation free energy*

The structural correlations observed in SO_2 loaded ILs have shown strong anion-SO_2 binding through multiple-site interactions. Thus, it is time to address the question of relative solubility of SO_2 in different anion-functionalized ILs. The free energy profiles for bringing one SO_2 molecule from its vapor phase into the bulk IL were determined. Figure 9 displays the free energy profiles for SO_2 solvation in various ILs containing $[P_{2221}]^+$ as the common cation but different anions. In an IL, the solvation free energy is the difference in free energies between the gas phase and the solvated state of SO_2. Moving in from the vapor phase, the SFE profiles become nonzero at around 52 Å in most ILs. However, in the case of $[P_{2221}]$[BrPhO], due to its smaller width

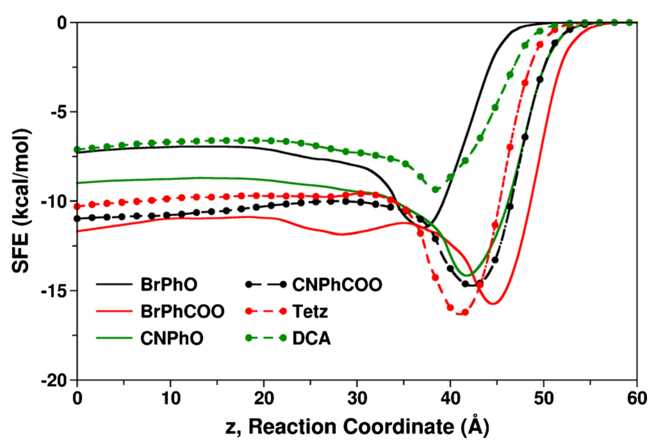

Figure 9. Solvation free energy profile of SO_2 in various IL ($[P_{2221}]^+$ as common cation). $z = 0$ is the center of mass of IL (bulk) and $z > 45$ is SO_2 in vapor phase.

of the density profile at the liquid-vapor interface (see Figure S9 in SI), such changes occur at 48 Å. The potential of mean force (PMF) attains a minimum around the interface and then starts to increase toward the bulk region. After crossing a barrier, it eventually converges to a constant value. Dang *et al.*, observed similar features in the PMF profile for CO_2 molecules across the air-IL interface.[59,64,89] In all the systems studied here, the PMF is most negative at the vapor-IL interface; thus, at low concentrations, SO_2 prefers to be located at the interface than in the bulk. A similar phenomenon has been reported for CO_2 by Perez-Blanco and Maginn.[63] The behavior of PMF across the air-IL interface has been compared with the number density profile of various sites on cation and anion in Figure 10. The preferred interaction of SO_2 with H_C and H_P atoms of the cation is confirmed by the occurrence of the minimum in SO_2 PMF and maximum in C_T number density at the interface.[60]

The decomposition of solvation free energy into its enthalpic and entropic contributions is crucial to interpret its anion dependence. Thus, in order to dissect the contributions to the total free energy profile, two additional simulations were performed. In one, the solute SO_2 molecule was immersed inside the bulk IL. In the other set up, the SO_2 molecule was kept in the vapor phase, *i.e.*, 50 Å apart from the bulk IL region. The simulation protocols used were the same as those described in free energy calculation section. Figure S10 (in SI) presents the potential energy in these two systems after an equilibration of 8 ns in the NVT ensemble. The change in enthalpy (ΔH) for SO_2 solvation in IL is deduced as the difference in potential energy between these two systems. The change in entropy (times the temperature) upon SO_2 solvation is quantified as the difference between solvation free energy and the potential energy, and the same is presented in Table 2. The entropy change due to solvation is moderate compared to the change in energy in these ILs. However, in ILs such as $[P_{2221}]$[BrPhCOO] and $[P_{2221}]$[CNPhCOO], the relative entropic contribution is slightly lower than in rest of the ILs; as a result, the net solvation free energy is a little high.

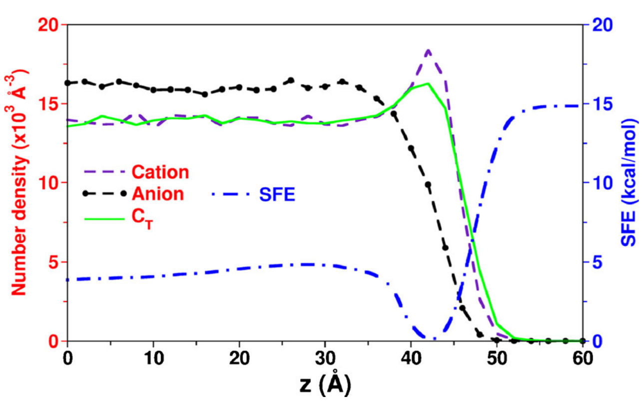

Figure 10. Number density profile of cation center of mass, anion center of mass and C_T atom of cation, compared against SO_2 solvation free energy profile in $[P_{2221}]$[CNPhCOO].

Further, Figure 11 displays the correlation between the computed SFE using empirical force field and molar volume of the respective ILs. For the sake of completeness, SO_2 solvation free energy has also been calculated in two other ILs, $[P_{2221}]$[PhO] and $[P_{2221}]$[PhCOO] and is tabulated in Table 2. It is evident from Table 2 that an inclusion of additional electronegative site at the para position not only reduces the binding energy (see Table 1) but also increases the net solvation free energy. This observation reaffirms the dual characteristics of the additional electron withdrawing groups (bromine or cyano) in this phenolate- and benzoate-based ILs. Among the ILs investigated here, $[P_{2221}]$[BrPhCOO] turned out to be the best solvent for SO_2 dissolution, as determined in experiment too.

Furthermore, Henry's law constant was calculated to obtain a quantitative measure of gas solubility in these ILs. It is defined as,

$$K_{\mathrm{H}} = \frac{RT\rho}{M} \exp\left(\frac{\Delta G}{RT}\right) \tag{2}$$

Table 2. Changes in free energy ($\Delta G = G_{liq} - G_{gas}$), enthalpy ($\Delta H = H_{liq} - H_{gas}$), and entropy ($T\Delta S = S_{liq} - S_{gas}$) for SO_2 solvation in various ILs. ΔS is a derived quantity from ΔG and ΔH. $[P_{2221}]^+$ is the cation.

Ionic liquid	ΔG (kcal/mol)	ΔH (kcal/mol)	TΔS (kcal/mol)
$[P_{2221}]$[BrPhO]	−7.04	−45.38	−38.34
$[P_{2221}]$[BrPhCOO]	−11.21	−32.75	−21.54
$[P_{2221}]$[CNPhO]	−8.79	−41.42	−32.63
$[P_{2221}]$[CNPhCOO]	−10.36	−35.16	−34.80
$[P_{2221}]$[Tetz]	−9.75	−46.28	−36.53
$[P_{2221}]$[DCA]	−6.10	−40.16	−34.06
$[P_{2221}]$[PhO]	−6.35	–	–
$[P_{2221}]$[PhCOO]	−9.45	–	–

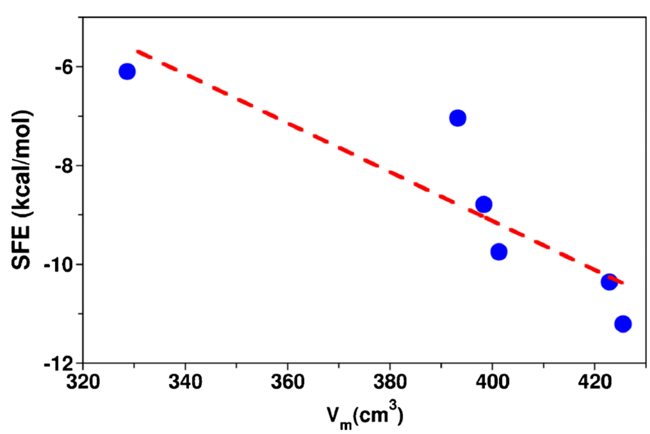

Figure 11. Molar volume of pure IL versus the solvation free energy (SFE) of SO_2 in bulk IL. Dashed line is the best fit to data.

Table 3. Henry's law constant (K_H) of SO_2 in studied ILs at 298 K and P = 1 atm.

Ionic liquid	$K_H \times 10^3$ (atm)
$[P_{2221}]$[BrPhO]	0.6989
$[P_{2221}]$[BrPhCOO]	0.0006
$[P_{2221}]$[CNPhO]	0.0366
$[P_{2221}]$[CNPhCOO]	0.0024
$[P_{2221}]$[Tetz]	0.0092
$[P_{2221}]$[DCA]	4.1450

where, ρ and M are the density and molecular weight of pure IL, and ΔG is the free energy changes due to solvation. The gas solubility in a liquid at infinite dilution is inversely proportional to the Henry's constant. Table 3 summarizes the computed Henry's law constant of SO_2 in all the IL systems studied here. From Figure 9 and Table 3, it is evident that SO_2 is very much soluble in these anion-functionalized ILs. The calculated K_H values demonstrate the following solubility order: $[BrPhCOO]^- > [CNPhCOO]^- > [Tetz]^- > [CNPhO]^- > [BrPhO]^- > [DCA]^-$. The obtained solubility order from free energy calculations is in good agreement with the experimentally measured SO_2 absorption capacities in these ILs ($[BrPhCOO]^- > [CNPhCOO]^- > [Tetz]^- > [CNPhO]^- > [BrPhO]^- > [DCA]^-$).[39,41,42]

4. Conclusions

In summary, we have provided detailed insights into the SO_2 solubility in anion-functionalized task-specific ILs from *ab initio* calculations and molecular dynamics simulations. Gas phase quantum chemical calculations show that in the presence of electron-withdrawing moiety such as bromine or cyano group, the negative charge on oxygen atom (in phenoxide or benzoate anion) get dispersed which results in a reduction in the interaction between oxygen atoms and SO_2, and thus, the binding energy (or absorption enthalpy) decreases. Moreover, due to the flow of negative charge from oxygen atoms to these additional sites, the negative charge on cyano nitrogen or bromine atom increases, which leads to enhanced CN/Br...SO_2 interaction. In the case of $[Tetz]^-$, besides $N_B \ldots SO_2$ interaction, oxygen atoms of SO_2 molecule form a strong hydrogen bond with H_A site. Thus, an improved absorption capacity at much lower desorption cost is a consequence of the dual role of the added interaction site on the anion.

MD simulations of bulk SO_2–IL mixtures indicated the propensity of both cation and anion to interact with the solute SO_2 molecule. The SO_2 molecule was found to interact with cations *via* dispersion forces, mainly with H_C and H_P hydrogens on the alkyl group. The cyano group exhibited stronger interaction with SO_2 molecule than the bromine site. The PMF profiles for SO_2 solvation obtained from ABF calculations manifested the air-IL interface to be a preferable location for the solute SO_2 molecule. The experimentally determined solubility of SO_2 in ILs varies as $[BrPhCOO]^- > [CNPhCOO]^- > [Tetz]^- > [CNPhO]^- > [BrPhO]^- > [DCA]^-$.[39,41,42] Solvation free energy values computed in this work are consistent with the experimental observations and anion site contributions to the free energy of solvation have been delineated.

Supplementary Information (SI)

The Supplementary Information associated with this article contains density of pure ILs, simulation box lengths, reaction coordinate, RDFs, CDFs, density profile and potential energy. Supplementary Information is available at http://www.ias.ac.in/chemsci.

Acknowledgements

We thank Department of Science and Technology, India for financial support.

References

1. Smith S J, van Aardenne J, Klimont Z, Andres R J, Volke A and Delgado A S 2011 Anthropogenic sulfur dioxide emissions: 1850–2005 *Atmos. Chem. Phys.* **11** 1101
2. Huang J, Riisager A, Wasserscheid P and Fehrmann R 2006 Reversible physical absorption of SO_2 by ionic liquids *Chem. Commun.* **38** 4027
3. Zheng Y, Kiil S and Johnsson J E 2003 Experimental investigation of a pilot-scale jet bubbling reactor for wet flue gas desulphurisation *Chem. Eng. Sci.* **58** 4695
4. Ma X, Kaneko T, Tashimo T, Yoshida T and Kato K 2000 Use of limestone for SO_2 removal from flue gas in the semidry FGD process with a powder-particle spouted bed *Chem. Eng. Sci.* **55** 4643
5. Dupont J, de Souza R F and Suarez P A Z 2002 Ionic liquid (molten salt) phase organometallic catalysis *Chem. Rev.* **102** 3667
6. Bates E D, Mayton R D, Ntai I and Davis J H 2002 CO_2 capture by a task-specific ionic liquid *J. Am. Chem. Soc.* **124** 926
7. Merrigan T L, Bates E D, Dorman S C and Davis J H 2000 New fluorous ionic liquids function as surfactants in conventional room-temperature ionic liquids *Chem. Commun.* 2051
8. Huang J-F, Luo H, Liang C, Sun I, Baker G A and Dai S 2005 Hydrophobic Brönsted acid-base ionic liquids

based on PAMAM dendrimers with high proton conductivity and blue photoluminescence *J. Am. Chem. Soc.* **127** 12784

9. Bara J E, Carlisle T K, Gabriel C J, Camper D, Finotello A, Gin D L and Noble R D 2009 Guide to CO_2 separations in imidazolium-based room-temperature ionic liquids *Ind. Eng. Chem. Res.* **48** 2739
10. Wang C, Luo H, -e Jiang D, Li H and Dai S 2010 Carbon dioxide capture by superbase-derived protic ionic liquids *Angew. Chem. Int. Ed.* **49** 5978
11. Xiong D, Cui G, Wang J, Wang H, Li Z, Yao K and Zhang S 2015 Reversible hydrophobic-hydrophilic transition of ionic liquids driven by carbon dioxide *Angew. Chem. Int. Ed.* **54** 7265
12. Wu W, Han B, Gao H, Liu Z, Jiang T and Huang J 2004 Desulfurization of flue gas: SO_2 absorption by an ionic liquid *Angew. Chem. Int. Ed.* **43** 2415
13. Anderson J L, Dixon J K, Maginn E J and Brennecke J F 2006 Measurement of SO_2 solubility in ionic liquids *J. Phys. Chem. B* **110** 15059
14. Hong S Y, Im J, Palgunadi J, Lee S D, Lee J S, Kim H S, Cheong M and Jung K-D 2011 Ether-functionalized ionic liquids as highly efficient SO_2 absorbents *Energy Environ. Sci.* **4** 1802
15. Prasad B R and Senapati S 2009 Explaining the differential solubility of flue gas components in ionic liquids from first-principle calculations *J. Phys. Chem. B* **113** 4739
16. Garcia G, Atilhan M and Aparicio S 2015 A density functional theory insight towards the rational design of ionic liquids for SO_2 capture *Phys. Chem. Chem. Phys.* **17** 13559
17. Yuan X L, Zhang S J and Lu X M 2007 Hydroxyl ammonium ionic liquids: Synthesis, properties, and solubility of SO_2 *J. Chem. Eng. Data* **52** 1150
18. Yokozeki A and Shiflett M B 2009 Separation of carbon dioxide and sulfur dioxide gases using room-temperature ionic liquid [hmim][Tf_2N] *Energy Fuels* **23** 4701
19. Shiflett M B and Yokozeki A 2010 Separation of carbon dioxide and sulfur dioxide using room-temperature ionic liquid [bmim][$MeSO_4$] *Energy Fuels* **24** 1001
20. Shiflett M B and Yokozeki A 2010 Chemical absorption of sulfur dioxide in room-temperature ionic liquids *Ind. Eng. Chem. Res.* **49** 1370
21. Yang D, Hou M, Ning H, Ma J, Kang X, Zhang J and Han B 2013 Reversible capture of SO_2 through functionalized ionic liquids *ChemSusChem* **6** 1191
22. Shang Y, Li H, Zhang S, Xu H, Wang Z, Zhang L and Zhang J 2011 Guanidinium-based ionic liquids for sulfur dioxide sorption *Chem. Eng. J.* **175** 324
23. Jiang Y-Y, Zhou Z, Jiao Z, Li L, Wu Y-T and Zhang Z-B 2007 SO_2 gas separation using supported ionic liquid membranes *J. Phys. Chem. B* **111** 5058
24. Luis P, Neves L, Afonso C, Coelhoso I, Crespo J, Garea A and Irabien A 2009 Facilitated transport of CO_2 and SO_2 through Supported ionic liquid membranes (SILMs) *Desalination* **245** 485
25. Hu X-B, Li Y-X, Huang K, Ma S-L, Yu H, Wu Y-T and Zhang Z-B 2012 Impact of α-d-glucose pentaacetate on the selective separation of CO_2 and SO_2 in supported ionic liquid membranes *Green Chem.* **14** 1440
26. Wang J, Zeng S, Bai L, Gao H, Zhang X and Zhang S 2014 Novel ether-functionalized pyridinium chloride ionic liquids for efficient SO_2 capture *Ind. Eng. Chem. Res* **53** 16832
27. Zeng S, He H, Gao H, Zhang X, Wang J, Huang Y and Zhang S 2015 Improving SO_2 capture by tuning functional groups on the cation of pyridinium-based ionic liquids *RSC Adv.* **5** 2470
28. Sun S, Niu Y, Xu Q, Sun Z and Wei X 2015 Highly efficient sulfur dioxide capture by glyme-lithium salt ionic liquids *RSC Adv.* **5** 46564
29. Han G-Q, Jiang Y-T, Deng D-S and Ai N 2015 Absorption of SO_2 by renewable ionic liquid/polyethylene glycol binary mixture and thermodynamic analysis *RSC Adv.* **5** 87750
30. Yang Z-Z, He L-N, Song Q-W, Chen K-H, Liu A-H and Liu X-M 2012 Highly efficient SO_2 absorption/activation and subsequent utilization by polyethylene glycol-functionalized Lewis basic ionic liquids *Phys. Chem. Chem. Phys.* **14** 15832
31. Wang C, Zheng J, Cui G, Luo X, Guo Y and Li H 2013 Highly efficient SO_2 capture through tuning the interaction between anion-functionalized ionic liquids and SO_2 *Chem. Commun.* **49** 1166
32. Wang C, Cui G, Luo X, Xu Y, Li H and Dai S 2011 Highly efficient and reversible SO_2 capture by tunable azole-based ionic liquids through multiple-site chemical absorption *J. Am. Chem. Soc.* **133** 11916
33. Huang J and Rüther T 2009 Why are ionic liquids attractive for CO_2 absorption? An overview *Aust. J. Chem.* **62** 298
34. Wang C, Luo X, Luo H, D-e Jiang, Li H and Dai S 2011 Tuning the basicity of ionic liquids for equimolar CO_2 capture *Angew. Chem. Int. Ed.* **50** 4918
35. Gurkan B, Goodrich B F, Mindrup E M, Ficke L E, Massel M, Seo S, Senftle T P, Wu H, Glaser M F and Shah J K 2010 Molecular design of high capacity, low viscosity, chemically tunable ionic liquids for CO_2 capture *J. Phys. Chem. Lett.* **1** 3494
36. Wang C, Luo H, Li H, Zhu X, Yu B and Dai S 2012 Tuning the physicochemical properties of diverse phenolic ionic liquids for equimolar CO_2 capture by the substituent on the anion *Chem. Eur. J.* **18** 2153
37. Teague C M, Dai S and en Jiang D 2010 Computational investigation of reactive to nonreactive capture of carbon dioxide by oxygen-containing lewis bases *J. Phys. Chem. A* **114** 11761
38. Cui G, Wang C, Zheng J, Guo Y, Luo X and Li H 2012 Highly efficient SO_2 capture by dual functionalized ionic liquids through a combination of chemical and physical absorption *Chem. Commun.* **48** 2633
39. Cui G, Zheng J, Luo X, Lin W, Ding F, Li H and Wang C 2013 Tuning anion-functionalized ionic liquids for improved SO_2 capture *Angew. Chem. Int. Ed.* **52** 10620
40. Cui G, Lin W, Ding F, Luo X, He X, Li H and Wang C 2014 Highly efficient SO_2 capture by phenyl-containing azole-based ionic liquids through multiple-site interactions *Green Chem.* **16** 1211
41. Cui G, Zhang F, Zhou X, Li H, Wang J and Wang C 2015 Tuning the basicity of cyano-containing ionic liquids to improve SO_2 capture through cyano-sulfur interactions *Chem. Eur. J.* **21** 5632

42. Chen K, Lin W, Yu X, Luo X, Ding F, He X, Li H and Wang C 2015 Designing of anion-functionalized ionic liquids for efficient capture of SO_2 from flue gas *AIChE J.* **61** 2028
43. Cui G, Huang Y, Zhang R, Zhang F and Wang J 2015 Highly efficient and reversible SO_2 capture by halogenated carboxylate ionic liquids *RSC Adv.* **5** 60975
44. Cui G, Zhang F, Zhou X, Huang Y, Xuan X and Wang 2015 Acylamido-based anion-functionalized ionic liquids for efficient SO_2 capture through multiple-site interactions *ACS Sustainable Chem. Eng.* **3** 2264
45. Cadena C, Anthony J L, Shah J K, Morrow T I, Brennecke J F and Maginn E J 2004 Why is CO_2 so soluble in imidazolium-based ionic liquids *J. Am. Chem. Soc.* **126** 5300
46. Huang X, Margulis C J, Li Y and Berne B J 2005 Why is the partial molar volume of CO_2 so small when dissolved in a room temperature ionic liquid? Structure and dynamics of CO_2 dissolved in [Bmim] [PF_6] *J. Am. Chem. Soc.* **127** 17842
47. Bhargava B L and Balasubramania S 2007 Insights into the structure and dynamics of a room-temperature ionic liquid: *Ab initio* molecular dynamics simulation studies of 1-*n*-Butyl-3-methylimidazolium hexafluorophosphate ([bmim][PF_6]) and the [bmim][PF_6]-CO_2 mixture *J. Phys. Chem. B* **111** 4477
48. Shah J and Maginn E J 2005 Monte carlo simulations of gas solubility in the ionic liquid 1-*n*-Butyl-3-methylimidazolium hexafluorophosphate *J. Phys. Chem. B* **109** 10395
49. Wang Y, Pan H, Li H and Wang C 2007 Force field of the TMGL ionic liquid and the solubility of SO_2 and CO_2 in the TMGL from molecular dynamics simulation *J. Phys. Chem. B* **111** 10461
50. Bhargava B L, Krishna A C and Balasubramanian S 2008 Molecular dynamics simulation studies of CO_2-[bmim][PF_6] solutions: Effect of CO_2 concentration *AIChE J.* **54** 2971
51. Zhang X, Huo F, Liu Z, Wang W, Shi W and Maginn E J 2009 Absorption of CO_2 in the ionic liquid 1-*n*-Hexyl-3-methylimidazolium tris(pentafluoroethyl)trifluorophosphate ([hmim][FEP]): A molecular view by computer simulations *J. Phys. Chem. B* **113** 7591
52. Zhang X, Liu X, Yao X and Zhang S 2011 Microscopic structure, interaction, and properties of a guanidinium-based ionic liquid and its mixture with CO_2 *Ind. Eng. Chem. Res.* **50** 8323
53. Monteiro M J, Ando R A, Siqueira L J A, Camilo F F, Santos P S, Ribeiro M C C and Torresi R M 2011 Effect of SO_2 on the transport properties of an imidazolium ionic liquid and its lithium solution *J. Phys. Chem. B* **115** 9662
54. Yu G and Chen X 2011 SO2 Capture by guanidinium-based ionic liquids: A theoretical study *J. Phys. Chem. B* **115** 3466
55. Ghobadi A F, Taghikhani V and Elliott J R 2011 Investigation on the solubility of SO_2 and CO_2 in imidazolium-based ionic liquids using NPT monte carlo simulation *J. Phys. Chem. B* **115** 13599
56. Mohammadi M and Foroutan M 2014 Molecular investigation of SO_2 gas absorption by ionic liquids: Effects of anion type *J. Mol. Liq.* **193** 60
57. Firaha D, Kavalchuk M and Kirchner B 2015 SO_2 solvation in the 1-ethyl-3-methylimidazolium thiocyanate ionic liquid by incorporation into the extended cation-anion network *J. Solution Chem.* **44** 838
58. Siqueira L J A, Ando R A, Bazito F F C, Torresi R M, Santos P S and Ribeiro M C C 2008 Shielding of ionic interactions by sulfur dioxide in an ionic liquid *J. Phys. Chem. B* **112** 6430
59. Wick C D, Chang T M and Dan L X 2010 Molecular mechanism of CO_2 and SO_2 molecules binding to the air/liquid interface of 1-butyl-3-methylimidazolium tetrafluoroborate ionic liquid: A molecular dynamics study with polarizable potential models *J. Phys. Chem. B* **114** 14965
60. Mondal A and Balasubramanian S 2016 Understanding SO_2 capture by ionic liquids *J. Phys. Chem. B* **120** 4457
61. Chandran A, Prakash K and Senapati S 2010 Self-Assembled inverted micelles stabilize ionic liquid domains in supercritical CO_2 *J. Am. Chem. Soc.* **132** 12511
62. Prakash P and Venkatnathan A 2016 Molecular mechanism of CO_2 absorption in phosphonium amino acid ionic liquid *RSC Adv.* **6** 55438
63. Perez-Blanco M E and Maginn E J 2001 Molecular dynamics simulations of CO_2 at an ionic liquid interface: Adsorption, ordering, and interfacial crossing *J. Phys. Chem. B* **114** 11827
64. Dang L X and Chang T-M 2012 Molecular mechanism of gas adsorption into ionic liquids: A molecular dynamics study *J. Phys. Chem. Lett.* **3** 175
65. Morganti J D, Hoher K, Ribeiro M C C, Ando R A and Siqueira L J 2014 Molecular dynamics simulations of acidic gases at interface of quaternary ammonium ionic liquids *J. Phys. Chem. C* **118** 22012
66. Frisch M J *et al.* 2009 Gaussian 09 Revision D.01. Gaussian Inc. Wallingford CT
67. Dennington R, Keith T and Millam J 2009 GaussView Version 5. Semichem Inc. Shawnee Mission KS
68. Boys S and Bernardi F 1970 The calculation of small molecular interactions by the differences of separate total energies. Some procedures with reduced errors *Mol. Phys.* **19** 553
69. Jeziorski B, Moszynski R and Szalewicz K 1994 Perturbation theory approach to intermolecular potential energy surfaces of van der Waals complexes *Chem. Rev.* **94** 1887
70. Turney J M *et al.* 2012 Psi4: An open-source ab initio electronic structure program *WIREs Comput. Mol. Sci.* **2** 556
71. Hohenstein E G and Sherrill C D 2010 Density fitting of intramonomer correlation effects in symmetry-adapted perturbation theory *J. Chem. Phys.* **133** 014101
72. Plimpton S 1995 Fast parallel algorithms for short-range molecular dynamics *J. Comput. Phys.* **117** 1
73. Wang Y-L, Shah F U, Glavatskih S, Antzutkin O N and Laaksonen A 2014 Atomistic insight into orthoborate-based ionic liquids: Force field development and evaluation *J. Phys. Chem. B* **118** 8711
74. Rai N and Siepmann J I 2007 Transferable potentials for phase equilibria. 9. explicit hydrogen description of benzene and five-membered and six-membered heterocyclic aromatic compounds *J. Phys. Chem. B* **111** 10790

75. Rai N and Siepmann J I 2013 Transferable potentials for phase equilibria. 10. explicit-hydrogen description of substituted benzenes and polycyclic aromatic compounds *J. Phys. Chem. B* **117** 273
76. Mondal A and Balasubramanian S 2014 Quantitative prediction of physical properties of imidazolium based room temperature ionic liquids through determination of condensed phase site charges: A refined force field *J. Phys. Chem. B* **118** 3409
77. Mondal A and Balasubramanian S 2015 A refined all-atom potential for imidazolium-based room temperature ionic liquids: Acetate, dicyanamide, and thiocyanate anions *J. Phys. Chem. B* **119** 11041
78. Ketko M H, Kamath G and Potoff J J 2011 Development of an optimized intermolecular potential for sulfur dioxide *J. Phys. Chem. B* **115** 4949
79. Martinez L, Andrade R, Birgin E G and Martinez J M 2009 PACKMOL: A package for building initial configurations for molecular dynamics simulations *J. Comp. Chem.* **30** 2157
80. Nosé S 1984 A unified formulation of the constant temperature molecular dynamics methods *J. Chem. Phys.* **81** 511
81. Hoover W G 1985 Canonical dynamics: Equilibrium phase-space distributions *Phys. Rev. A* **31** 1695
82. Humphrey W, Dalke A and Schulten K 1996 VMD: Visual molecular dynamics *J. Mol. Graphics* **14** 33
83. Fiorin G, Klein M L and Hénin J 2013 Using collective variables to drive molecular dynamics simulations *Mol. Phys.* **111** 3345
84. Darve E, Rodriguez-Gómez D and Pohorille A 2008 Adaptive biasing force method for scalar and vector free energy calculations *J. Chem. Phys.* **128** 144120
85. Sharma S, Gupta A, Dhabal D and Kashyap H K 2016 Pressure-dependent morphology of trihexyl(tetradecyl)phosphonium ionic liquids: A molecular dynamics study *J. Chem. Phys.* **145** 134506
86. Xing H, Liao C, Yang Q, Veith G M, Guo B, Sun X-G, Ren Q, Hu Y-S and Dai S 2014 Ambient Lithium-SO_2 batteries with ionic liquids as electrolytes *Angew. Chem. Int. Ed.* **53** 2099
87. Weber H, Salanne M and Kirchner B 2015 Toward an accurate modeling of ionic liquid-TiO_2 interfaces *J. Phys. Chem. C* **119** 25260
88. Brehm M, Weber H, Pensado A S, Stark A and Kirchner B 2012 Proton transfer and polarity changes in ionic liquid-water mixtures: A perspective on hydrogen bonds from *ab initio* molecular dynamics at the example of 1-ethyl-3-methylimidazolium acetate-water mixtures-Part 1 *Phys. Chem. Chem. Phys* **14** 5030
89. Dang L X and Wick C D 2011 Anion effects on interfacial absorption of gases in ionic liquids. A molecular dynamics study *J. Phys. Chem. B* **115** 6964